El Niño–Global Atmospheric Oscillation as the Main Mode of Interannual Climate Variability

Ilya V. Serykh [1,2,*] and Dmitry M. Sonechkin [1]

[1] Shirshov Institute of Oceanology, Russian Academy of Sciences, 117997 Moscow, Russia; dsonech@ocean.ru

[2] Geophysical Center, Russian Academy of Sciences, 119296 Moscow, Russia

[*] Correspondence: iserykh@ocean.ru

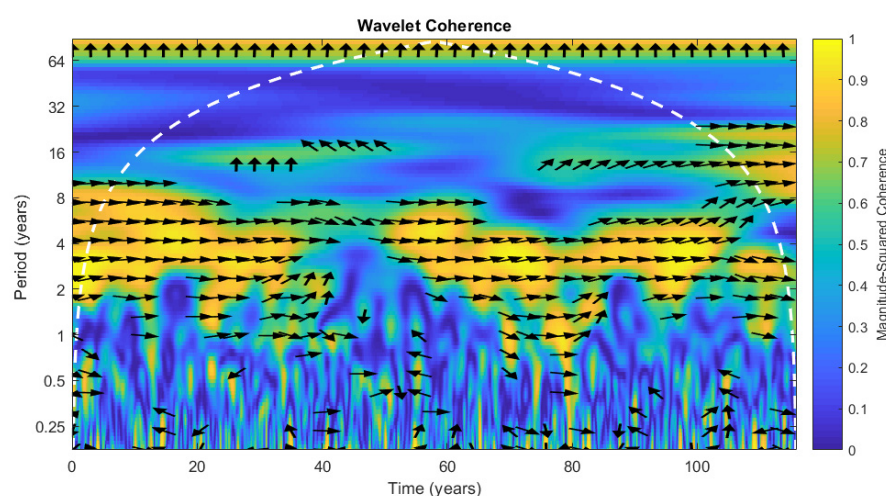**Figure S1.** The wavelet coherence and phase between GAO2 and EONI for 1900–2015. Phase from the wavelet cross-spectrum is indicated by arrows oriented in a particular direction to indicate the relative lag between coherent components in regions of the time-frequency plane where coherence exceeds 0.5. The white dashed line shows the cone of influence where edge effects become significant (95%).

Figure S2. The wavelet coherence and phase between GAO2 and TAS anomalies in Amundsen Sea region (55°-70°S, 150°-100°W) for 1900–2015. Phase from the wavelet cross-spectrum is indicated by arrows oriented in a particular direction to indicate the relative lag between coherent components in regions of the time-frequency plane where coherence exceeds 0.5. The white dashed line shows the cone of influence where edge effects become significant (95%).
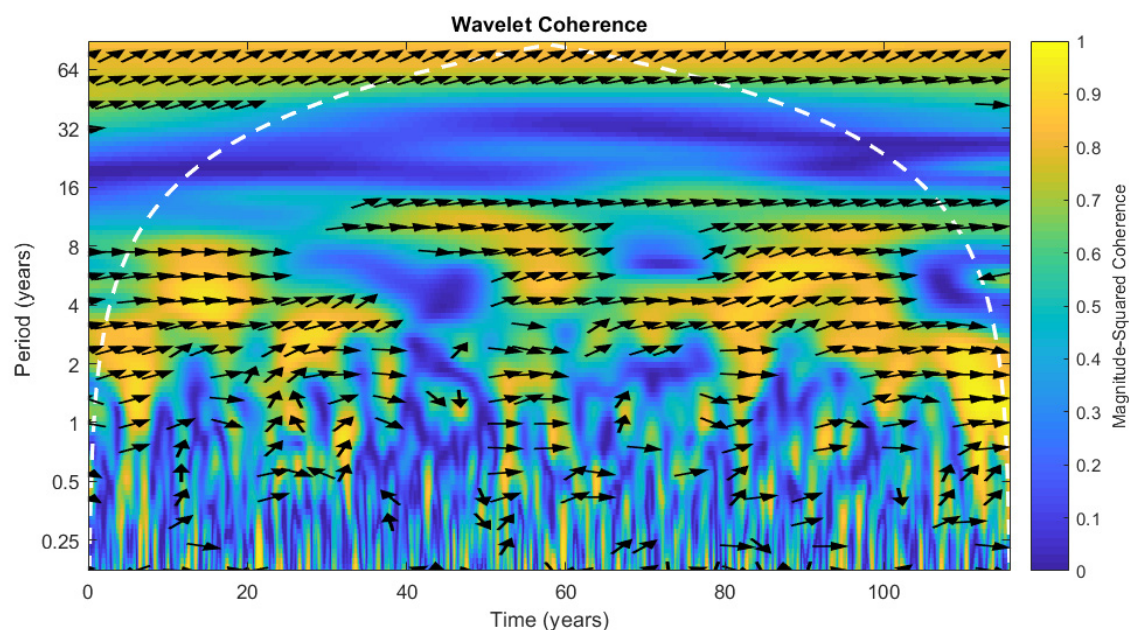

Figure S3. The wavelet coherence and phase between GAO2 and TAS anomalies in Alaska region (55°-70°N, 170°-120°W) for 1900–2015. Phase from the wavelet cross-spectrum is indicated by arrows oriented in a particular direction to indicate the relative lag between coherent components in regions of the time-frequency plane where coherence exceeds 0.5. The white dashed line shows the cone of influence where edge effects become significant (95%).
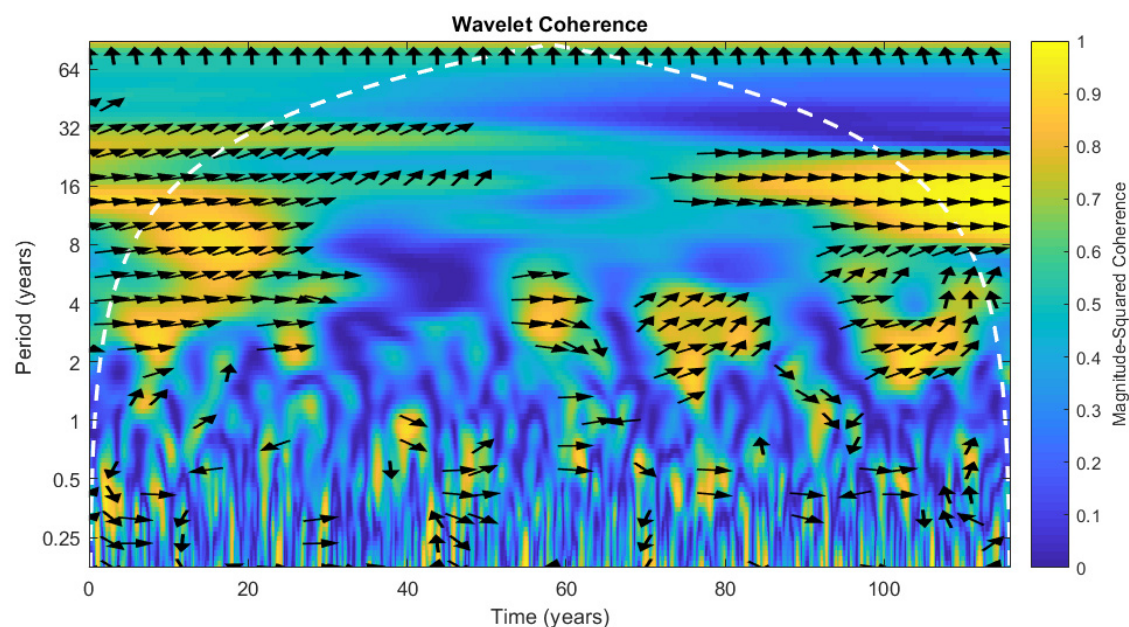
Figure S4. The wavelet coherence and phase between GAO2 and TAS anomalies in northern part of the western Pacific Ocean middle latitudes region (30°-45°N, 160°E-160°W) for 1900–2015. Phase from the wavelet cross-spectrum is indicated by arrows oriented in a particular direction to indicate the relative lag between coherent components in regions of the time-frequency plane where coherence exceeds 0.5. The white dashed line shows the cone of influence where edge effects become significant (95%).
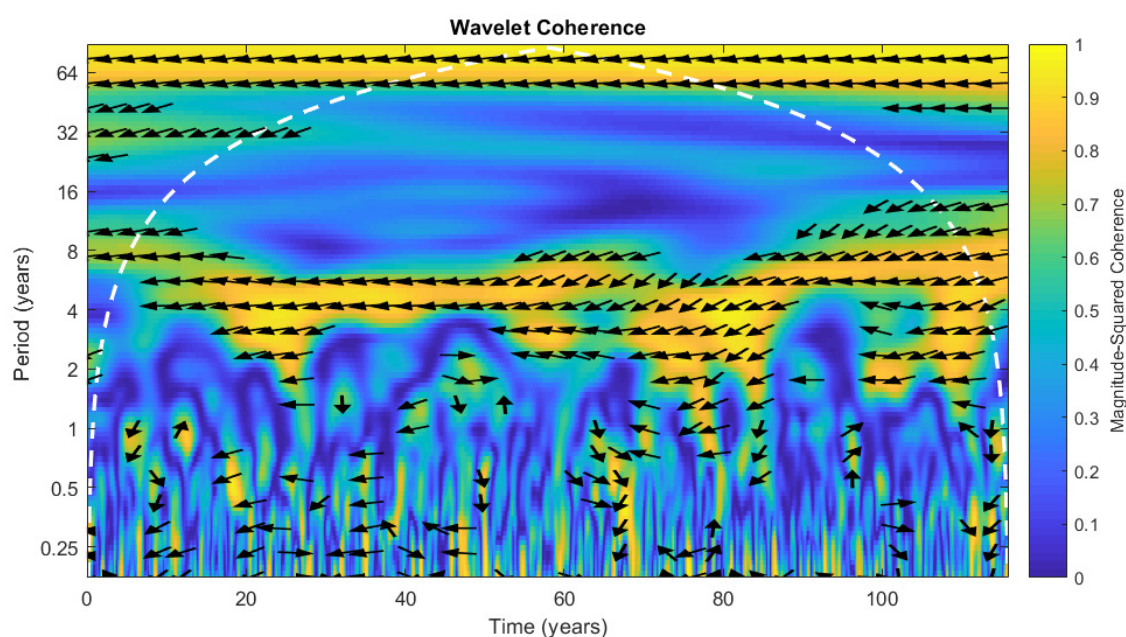

Figure S5. The wavelet coherence and phase between GAO2 and TAS anomalies in southern part of the western Pacific Ocean middle latitudes region (20°-35°S, 160°E-150°W) for 1900–2015. Phase from the wavelet cross-spectrum is indicated by arrows oriented in a particular direction to indicate the relative lag between coherent components in regions of the time-frequency plane where coherence exceeds 0.5. The white dashed line shows the cone of influence where edge effects become significant (95%).
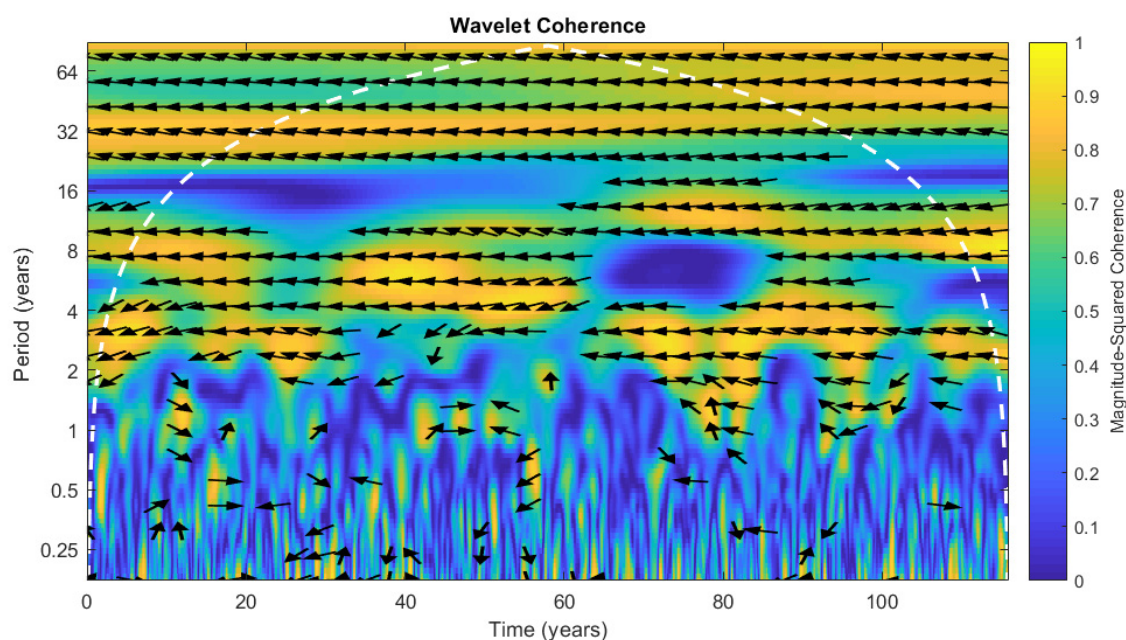
Figure S6. The wavelet coherence and phase between GAO2 and TAS anomalies in Indian Ocean region (0°-20°S, 50°-90°E) for 1900–2015. Phase from the wavelet cross-spectrum is indicated by arrows oriented in a particular direction to indicate the relative lag between coherent components in regions of the time-frequency plane where coherence exceeds 0.5. The white dashed line shows the cone of influence where edge effects become significant (95%).
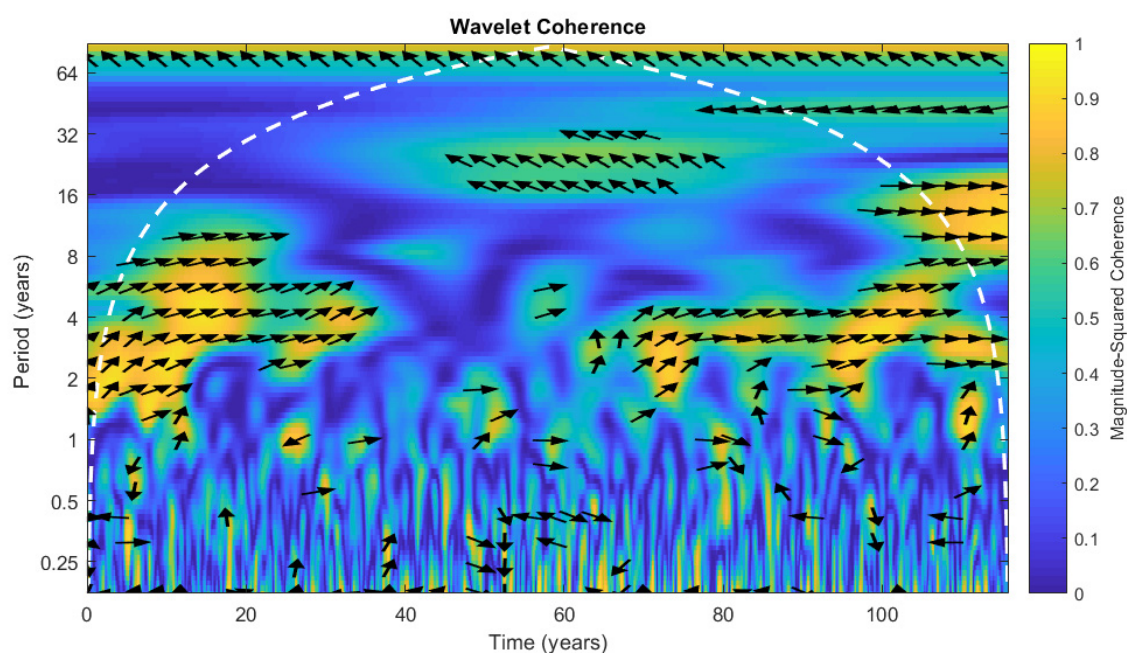

Figure S7. The wavelet coherence and phase between GAO2 and TAS anomalies in Hindustan Peninsula region (10°-30°N, 75°-85°E) for 1900–2015. Phase from the wavelet cross-spectrum is indicated by arrows oriented in a particular direction to indicate the relative lag between coherent components in regions of the time-frequency plane where coherence exceeds 0.5. The white dashed line shows the cone of influence where edge effects become significant (95%).
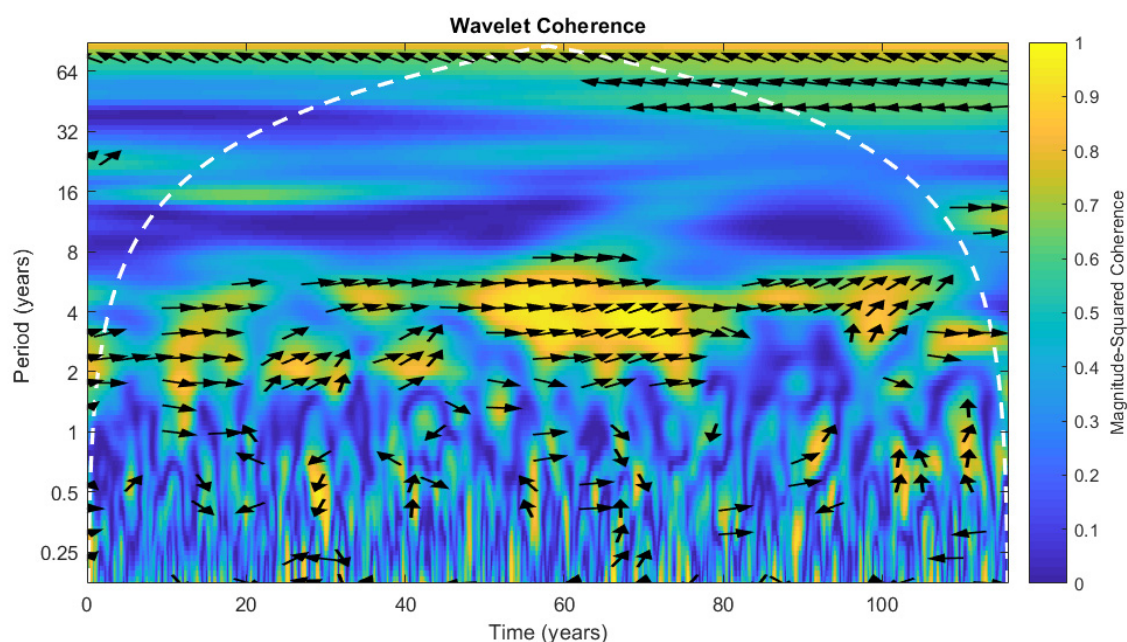
Figure S8. The wavelet coherence and phase between GAO2 and TAS anomalies in Australia region (20°-35°S, 120°-150°E) for 1900–2015. Phase from the wavelet cross-spectrum is indicated by arrows oriented in a particular direction to indicate the relative lag between coherent components in regions of the time-frequency plane where coherence exceeds 0.5. The white dashed line shows the cone of influence where edge effects become significant (95%).
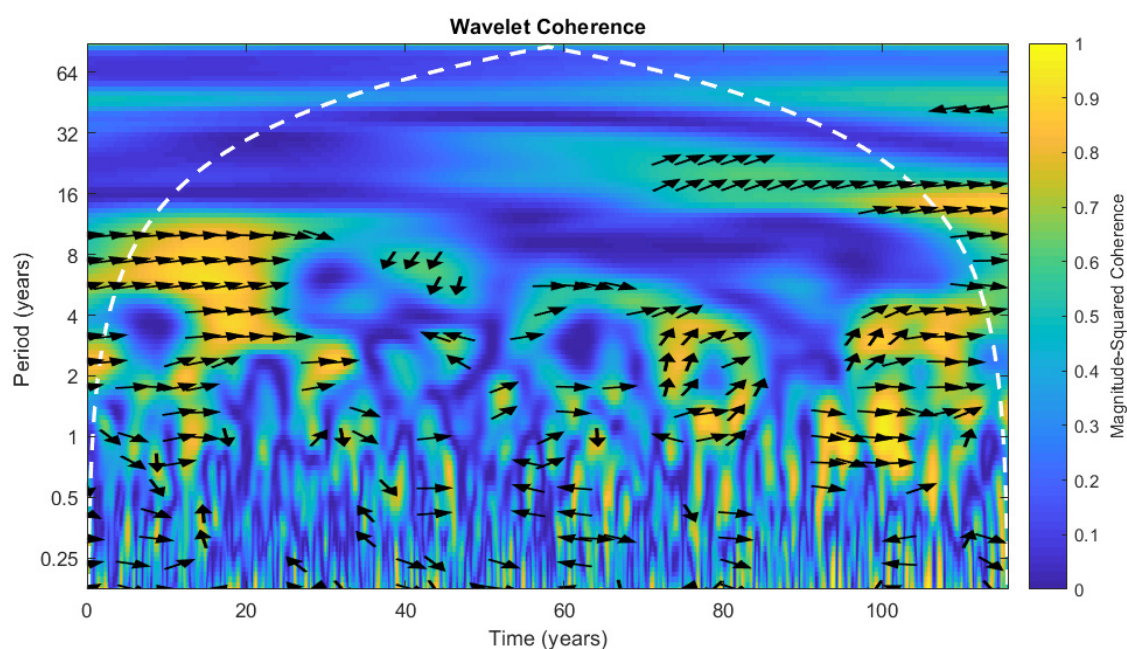

Figure S9. The wavelet coherence and phase between GAO2 and TAS anomalies in Southern Africa region (15°-30°S, 20°-30°E) for 1900–2015. Phase from the wavelet cross-spectrum is indicated by arrows oriented in a particular direction to indicate the relative lag between coherent components in regions of the time-frequency plane where coherence exceeds 0.5. The white dashed line shows the cone of influence where edge effects become significant (95%).
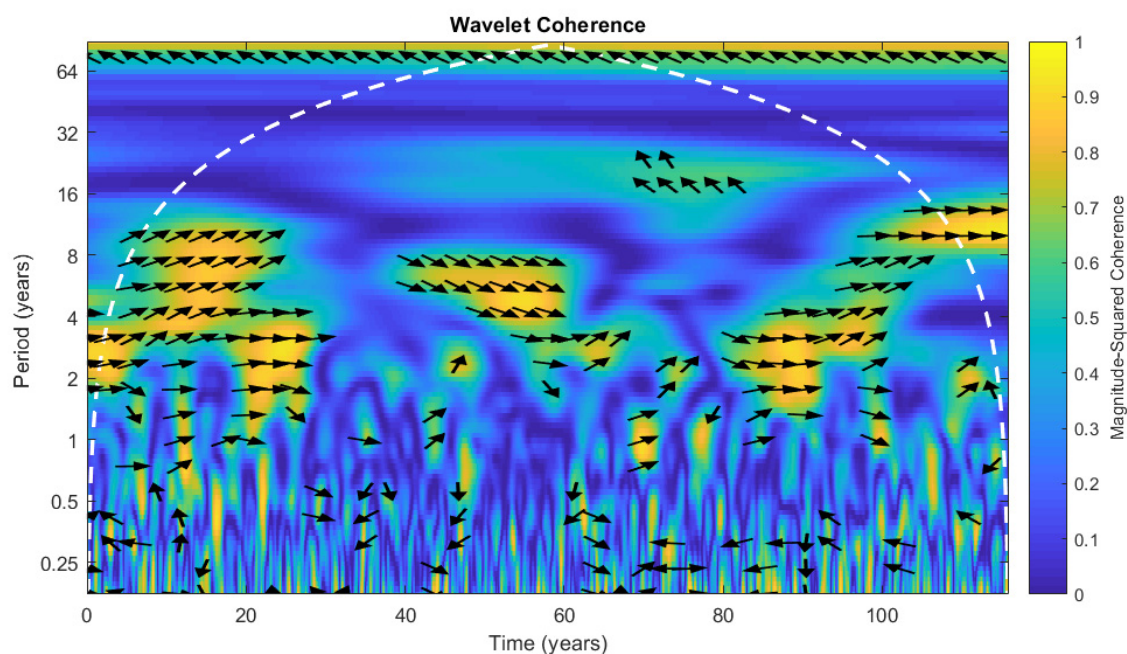
Figure S10. The wavelet coherence and phase between GAO2 and TAS anomalies in high latitudes of Southern Atlantic region (70°-60°S, 60°-30°W) for 1900–2015. Phase from the wavelet cross-spectrum is indicated by arrows oriented in a particular direction to indicate the relative lag between coherent components in regions of the time-frequency plane where coherence exceeds 0.5. The white dashed line shows the cone of influence where edge effects become significant (95%).
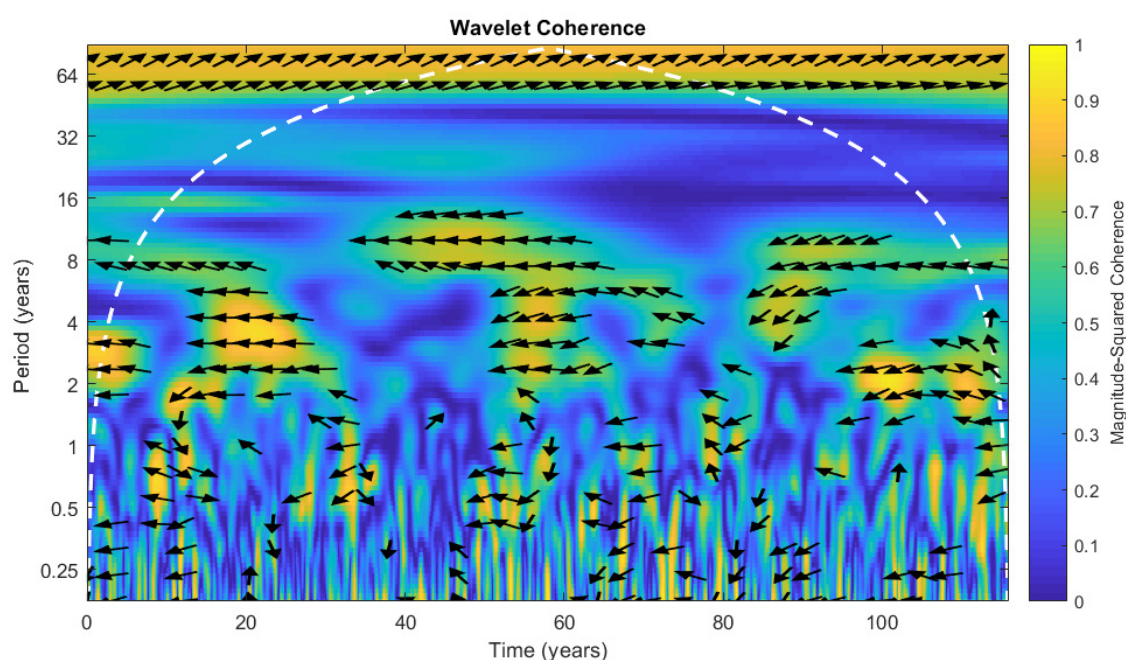
Figure S11. The wavelet coherence and phase between GAO2 and TAS anomalies in South American continent region (15°S-5°N, 70°-50°W) for 1900–2015. Phase from the wavelet cross-spectrum is indicated by arrows oriented in a particular direction to indicate the relative lag between coherent components in regions of the time-frequency plane where coherence exceeds 0.5. The white dashed line shows the cone of influence where edge effects become significant (95%).
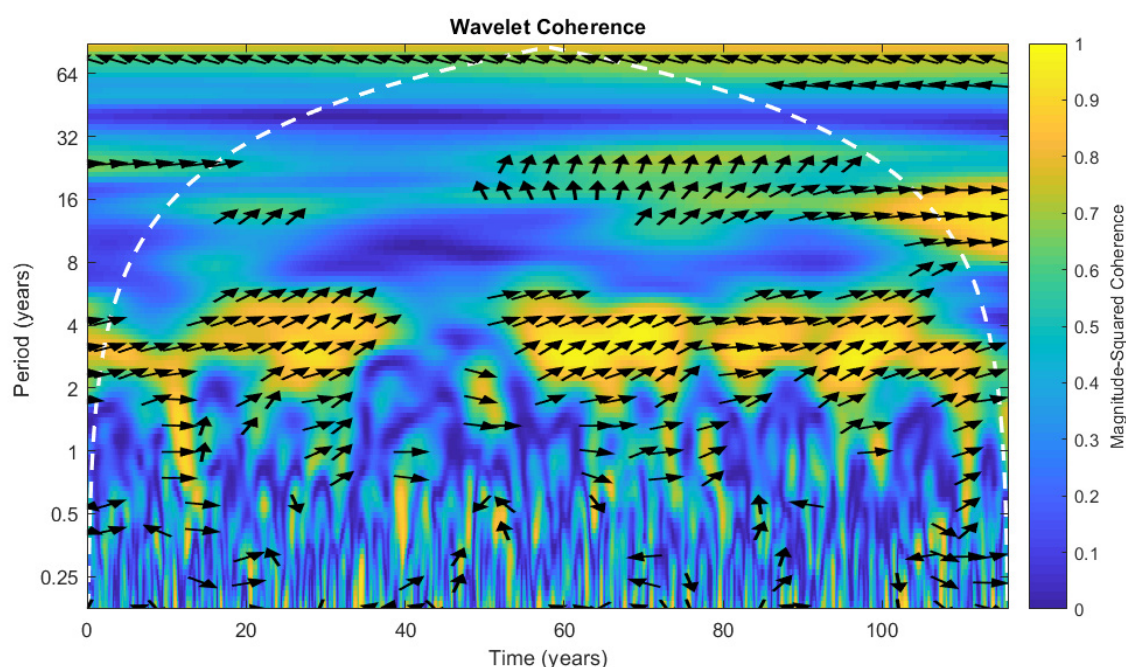
Figure S12. The wavelet coherence and phase between GAO2 and TAS anomalies in southern and eastern parts of North America region (25°-45°N, 105°-70°W) for 1900–2015. Phase from the wavelet cross-spectrum is indicated by arrows oriented in a particular direction to indicate the relative lag between coherent components in regions of the time-frequency plane where coherence exceeds 0.5. The white dashed line shows the cone of influence where edge effects become significant (95%).
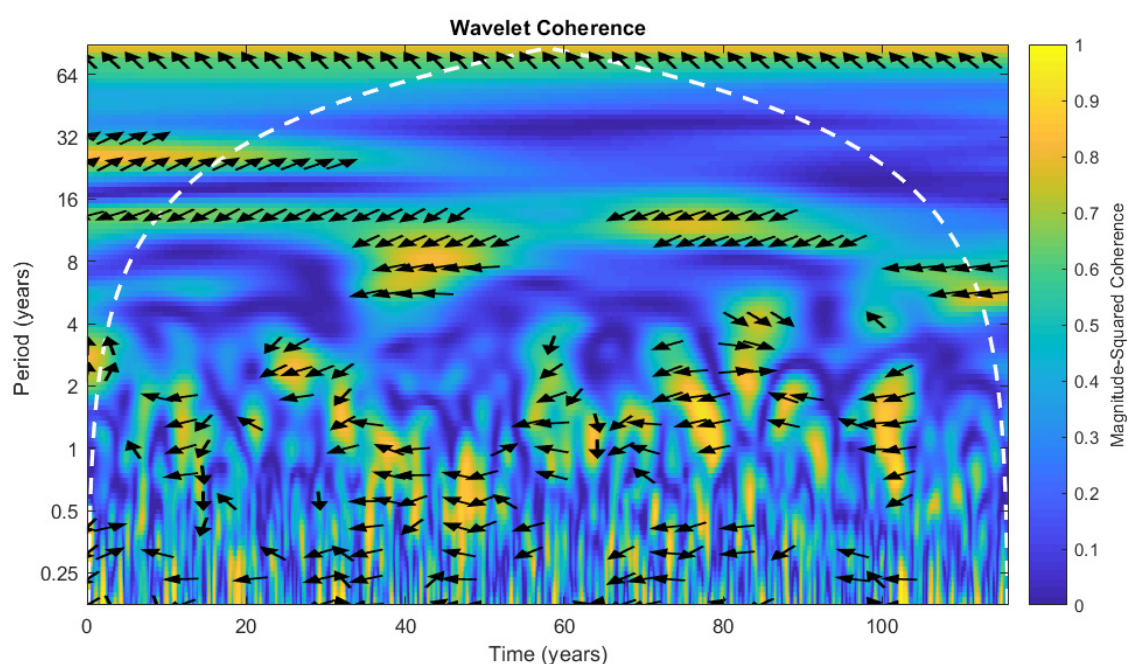

Figure S13. The wavelet coherence and phase between GAO2 and TAS anomalies in the northern part of Eurasia and the Arctic region (60°-80°N, 10°-150°E) for 1900–2015. Phase from the wavelet cross-spectrum is indicated by arrows oriented in a particular direction to indicate the relative lag between coherent components in regions of the time-frequency plane where coherence exceeds 0.5. The white dashed line shows the cone of influence where edge effects become significant (95%).
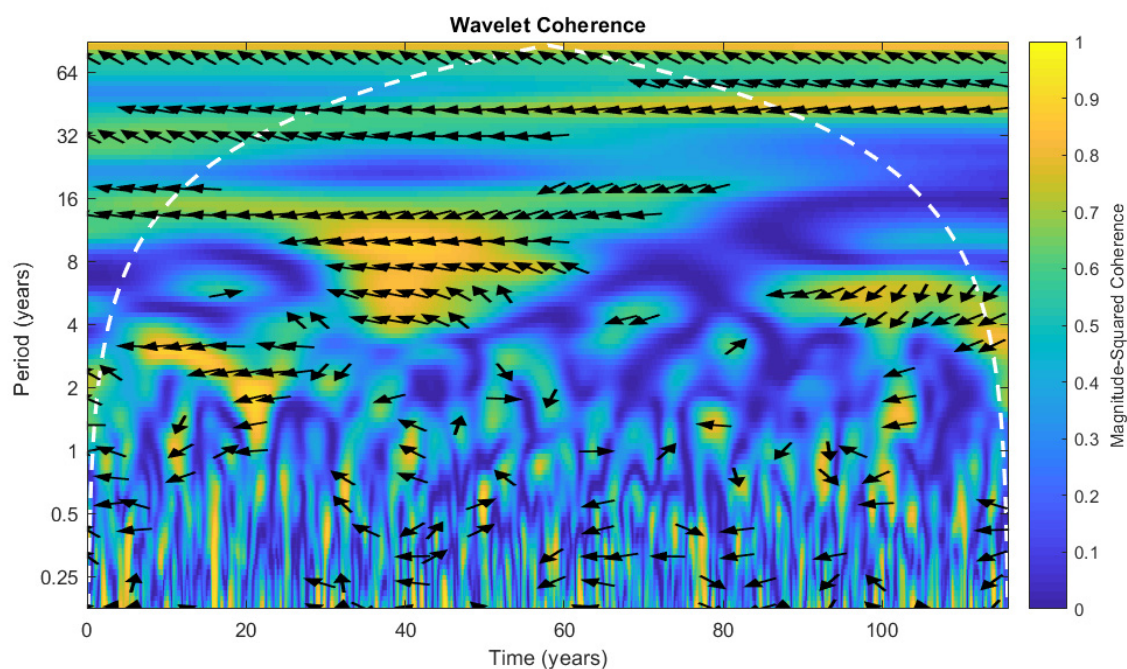
Figure S14. The wavelet coherence and phase between GAO2 and TAS anomalies in Black and Caspian Seas region (35°-45°N, 25°-50°E) for 1900–2015. Phase from the wavelet cross-spectrum is indicated by arrows oriented in a particular direction to indicate the relative lag between coherent components in regions of the time-frequency plane where coherence exceeds 0.5. The white dashed line shows the cone of influence where edge effects become significant (95%).
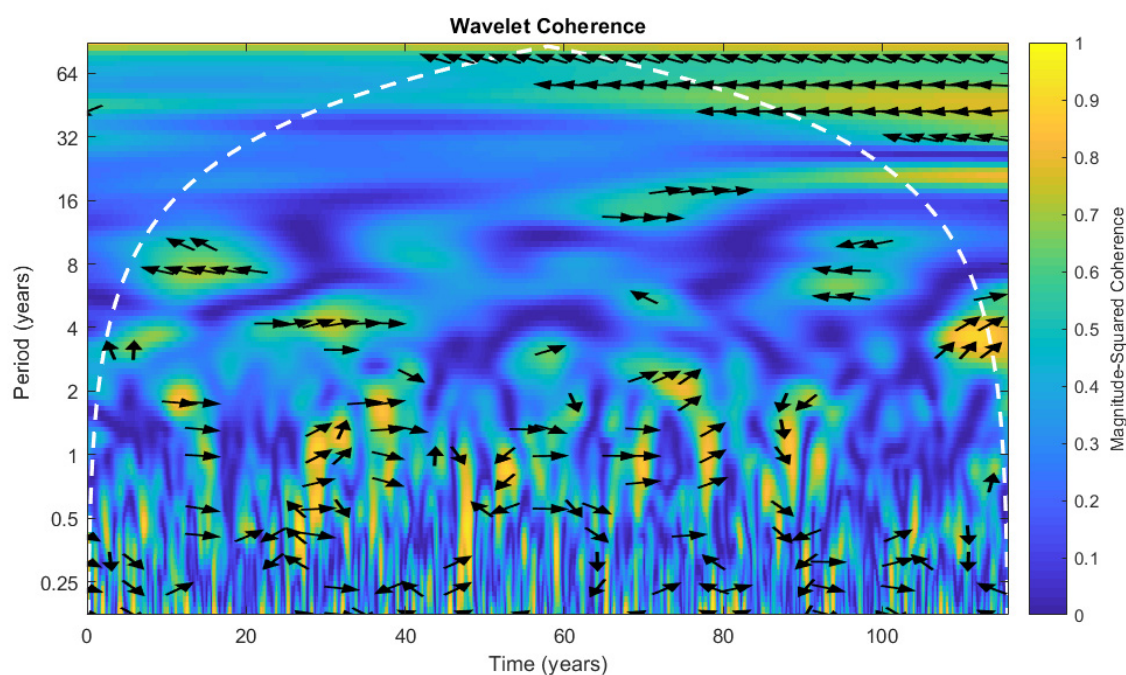

Figure S15. The wavelet coherence and phase between GAO2 and SLP anomalies in the low latitudes of South America, the Atlantic Ocean, Africa, the Indian Ocean region, the Indonesian archipelago, Australia, and the western part of the Pacific Ocean region (30°S-30°N, 50°W-170°E) for 1900–2015. Phase from the wavelet cross-spectrum is indicated by arrows oriented in a particular direction to indicate the relative lag between coherent components in regions of the time-frequency plane where coherence exceeds 0.5. The white dashed line shows the cone of influence where edge effects become significant (95%).
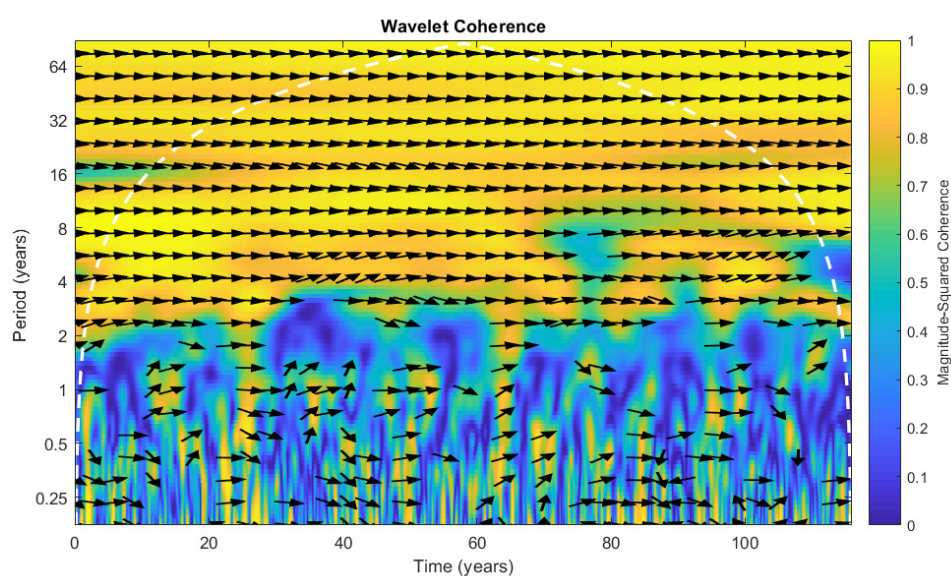
Figure S16. The wavelet coherence and phase between GAO2 and SLP anomalies in middle latitudes of the northern part of Pacific Ocean region (45°-55°N, 175°-165°W) for 1900–2015. Phase from the wavelet cross-spectrum is indicated by arrows oriented in a particular direction to indicate the relative lag between coherent components in regions of the time-frequency plane where coherence exceeds 0.5. The white dashed line shows the cone of influence where edge effects become significant (95%).
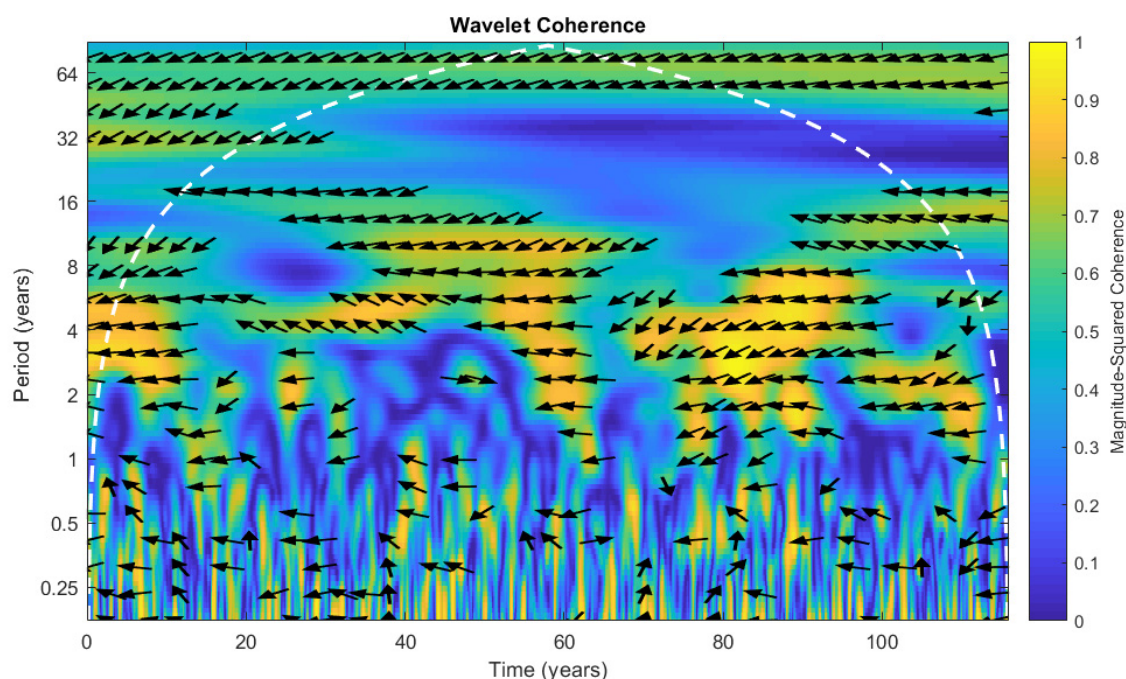

Figure S17. The wavelet coherence and phase between GAO2 and SLP anomalies in middle latitudes of the southern part of Pacific Ocean region (55°-45°S, 175°-165°W) for 1900–2015. Phase from the wavelet cross-spectrum is indicated by arrows oriented in a particular direction to indicate the relative lag between coherent components in regions of the time-frequency plane where coherence exceeds 0.5. The white dashed line shows the cone of influence where edge effects become significant (95%).
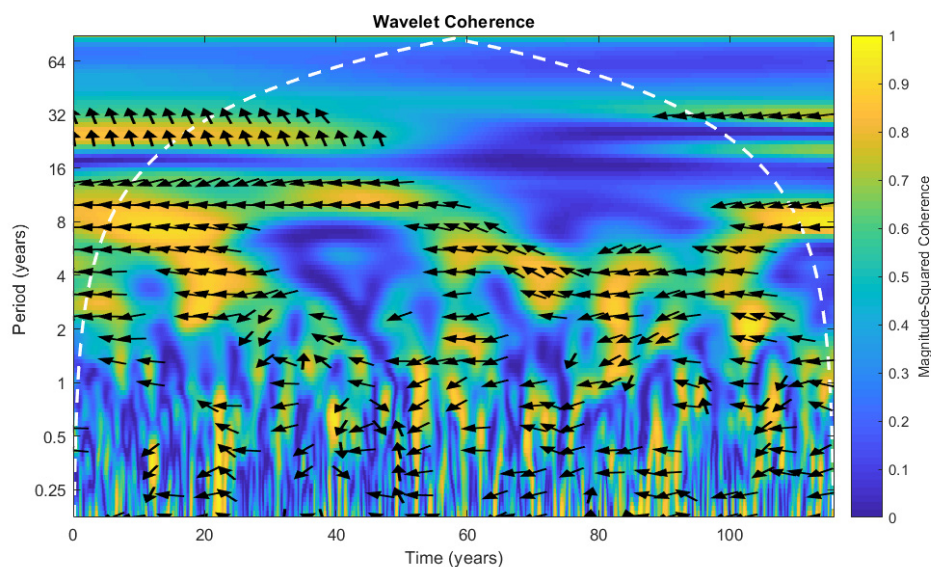
Figure S18. The wavelet coherence and phase between GAO2 and SLP anomalies in middle latitudes of the northern part of Atlantic Ocean region (45°-55°N, 15°-5°W) for 1900–2015. Phase from the wavelet cross-spectrum is indicated by arrows oriented in a particular direction to indicate the relative lag between coherent components in regions of the time-frequency plane where coherence exceeds 0.5. The white dashed line shows the cone of influence where edge effects become significant (95%).
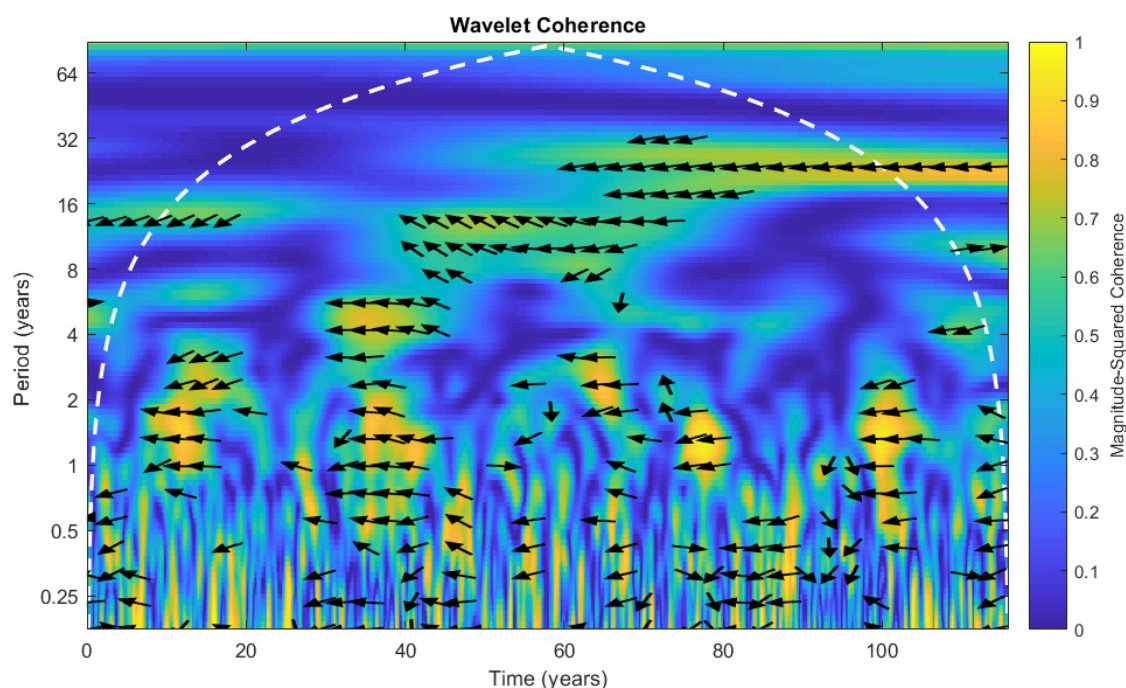

Figure S19. The wavelet coherence and phase between GAO2 and SLP anomalies in middle latitudes of the southern part of Atlantic Ocean region (55°-45°S, 15°-5°W) for 1900–2015. Phase from the wavelet cross-spectrum is indicated by arrows oriented in a particular direction to indicate the relative lag between coherent components in regions of the time-frequency plane where coherence exceeds 0.5. The white dashed line shows the cone of influence where edge effects become significant (95%).
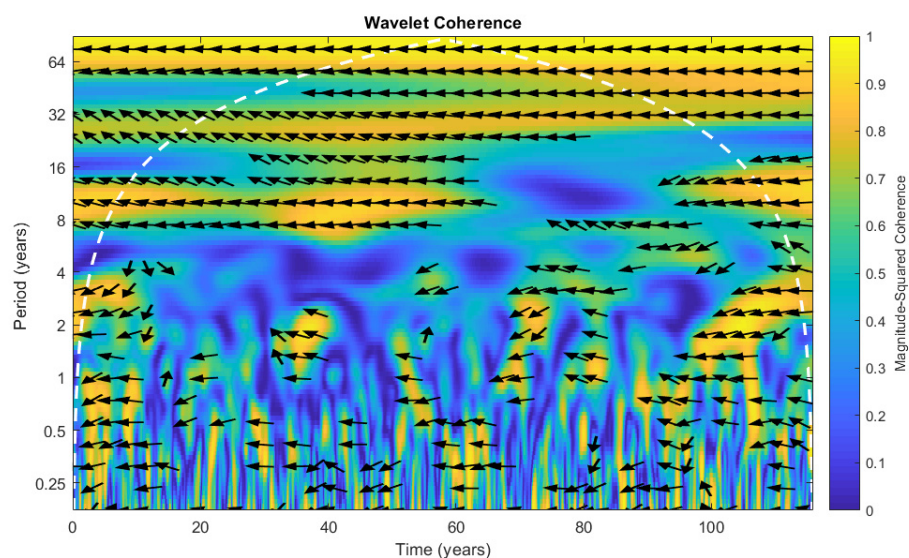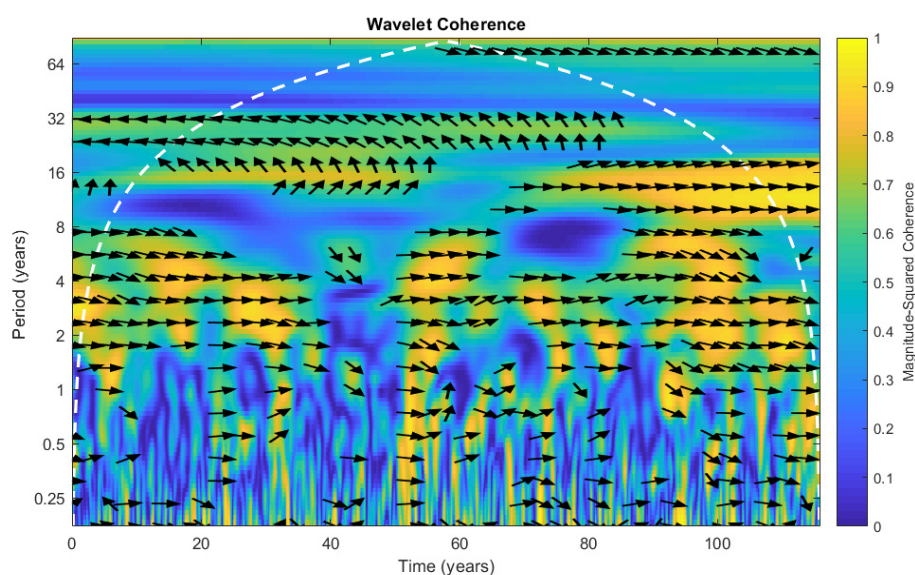
Figure S20. The wavelet coherence and phase between GAO2 and SLP anomalies in the Amundsen, Bellingshausen and Weddell Seas region (70°-55°S, 130°-70°W) for 1900–2015. Phase from the wavelet cross-spectrum is indicated by arrows oriented in a particular direction to indicate the relative lag between coherent components in regions of the time-frequency plane where coherence exceeds 0.5. The white dashed line shows the cone of influence where edge effects become significant (95%).
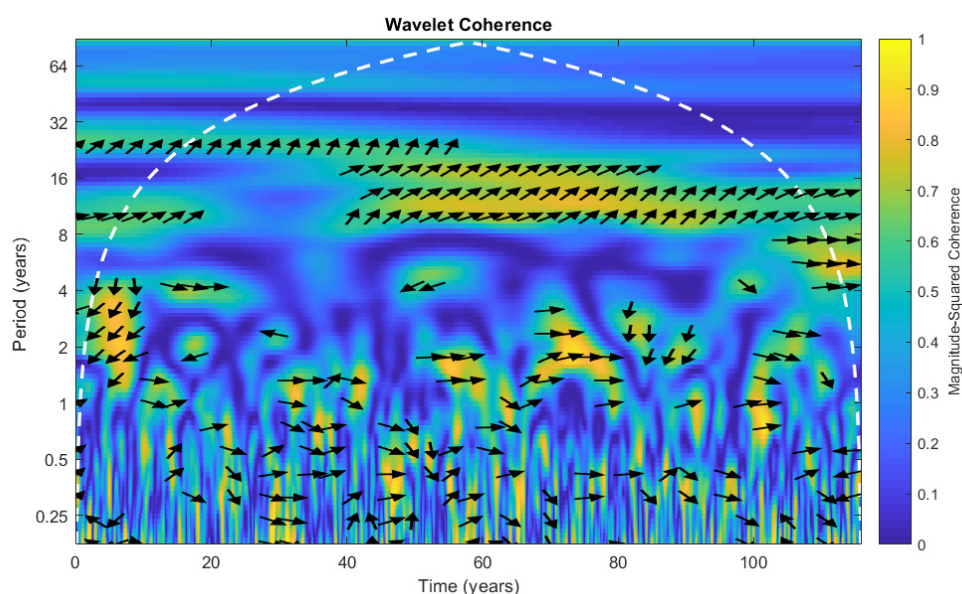

Figure S21. The wavelet coherence and phase between GAO2 and SLP anomalies in the North America region (40°-70°N, 110°-80°W) for 1900–2015. Phase from the wavelet cross-spectrum is indicated by arrows oriented in a particular direction to indicate the relative lag between coherent components in regions of the time-frequency plane where coherence exceeds 0.5. The white dashed line shows the cone of influence where edge effects become significant (95%).